Enhancing soil vapor extraction with EKSF for the removal of HCHs

João Miller de Melo Henrique [a,b], Julia Isidro [b], Cristina Sáez [b], Rubén López-Vizcaíno [c], Angel Yustres [c], Vicente Navarro [c], Elisama V. Dos Santos [a], Manuel A. Rodrigo [b,*]

[a] Postgraduate Program in Chemical Engineering, School of Science and Technology, Federal University of Rio Grande do Norte, 59078-970, Natal, RN, Brazil
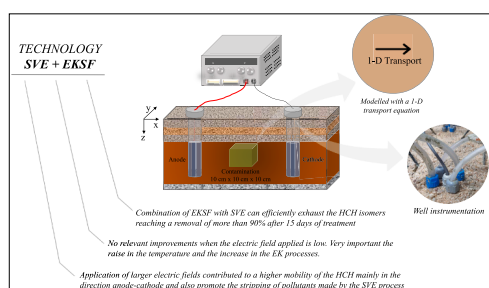[b] Department of Chemical Engineering, Faculty of Chemical Sciences & Technologies, Universidad de Castilla La Mancha, Campus Universitario, s/n, 13071, Ciudad Real, Spain
[c] Geoenvironmental Group, Civil Engineering School, University of Castilla-La Mancha, Avda. Camilo José Cela s/n, 13071, Ciudad Real, Spain

HIGHLIGHTS

- EKSF combined with SVE can remove more than 90% of HCH from soil in 15 days.
- Electric field of 3 Vcm^{-1} improves the efficiencies of the combined treatment efficiency.
- Electrolyte wells allows to keep water content in suitable values.
- Good fitting of experimental results to a 1-D transport model.
- Volatilization process is the primary in the combined EKSF-SVE.

GRAPHICAL ABSTRACT

TECHNOLOGY SVE + EKSF

1-D Transport

Modelled with a 1-D transport equation

Well instrumentation

Combination of EKSF with SVE can efficiently exhaust the HCH isomers reaching a removal of more than 90% after 15 days of treatment

No relevant improvements when the electric field applied is low. Very important the raise in the temperature and the increase in the EK processes.

Application of larger electric fields contributed to a higher mobility of the HCH mainly in the direction anode-cathode and also promote the stripping of pollutants made by the SVE process

ARTICLE INFO

ABSTRACT

This paper evaluates the combination of electrokinetic soil flushing (EKSF) with soil vapor extraction (SVE) for the removal of four hexachlorocyclohexane (HCH) isomers contained in a real matrix. Results demonstrate that the combination of EKSF and SVE can be positive, but it is required the application of high electric fields (3 V cm^{-1}) in order to promote a higher temperature in the system, which improves the volatilization of the HCH contained in the system. Electrokinetic transport is also enhanced with the application of higher electric gradients, but these transport processes are slower than the volatilization processes, which are the primary in this system. Hence collection of species in the electrolyte wells is negligible as compared to the compound dragged with air by the SVE but the temperature increase demonstrates a good performance. Combination of EKSF with SVE can efficiently exhaust the four HCH isomers reaching a removal of more than 90% after 15 days of treatment (20% more than values attained by SVE) but it is required the application of high electric fields to promote a higher temperature in the system (to improve the volatilization) and EK transport (to improve the dragging). 1-D transport model can be easily used to estimate the average pore water velocity and the effective diffusion of each compound under the different experimental conditions tested.

Novelty statement

This research evaluates the combination of electrokinetic soil flushing (EKSF) with soil vapor extraction (SVE) for the removal in pilot-scale of four hexachlorocyclohexane isomers contained in a real matrix. Performance of EKSF with and without electrodes polarity reversal (1.0 Vcm^{-1}) and applying two electric fields (1.0 and 3.0 Vcm^{-1}) were compared. Combination of EKSF with SVE can efficiently exhaust the isomers reaching a removal of more than 90% after 15 days. These values are only of 70% when SVE alone is applied. No relevant improvements when the electric gradient applied is low. Volatilization processes are the primary in this system.

1. Introduction

Contamination of soil with hexachlorocyclohexane (HCH) isomers is a worldwide environmental concern. Among the HCHs isomers, lindane has been extensively used as a pesticide until the 1990s. Different process have been developed for the remediation of the contaminated soil, including chemical oxidation (Usman et al., 2014, 2017; Dominguez et al., 2021) chemical reduction (Chen et al., 2020), electrochemical (Munoz-Morales et al., 2017; Vidal et al., 2020), biological (Phillips et al., 2005) and thermal processes (Minghui et al., 1996; Araújo et al., 2016), in addition to the association of these technologies to improve the efficiency of removal of contaminants from soils.

Among the different technologies studied, the electrokinetic soil flushing (EKSF) consists of the mobilization of flushing fluids by electrokinetic processes in polluted soils, with the purpose of dragging the pollutants contained in soil to electrode wells, producing a spent flushing fluid from which pollution is later treated (Virkutyte et al., 2002; Rodrigo et al., 2014a; dos Santos et al., 2016; Hahladakis et al., 2016; Risco et al., 2016; Liu et al., 2020; Rodrigo and dos Santos, 2020; Song et al., 2021). This process uses the application of an electric field generated by electrodes located on the subsurface, producing a voltage gradient responsible for transport mechanisms (electroosmosis, electromigration and electrophoresis) (Virkutyte et al., 2002; Gomes et al., 2012; Rodrigo et al., 2014b; Cameselle and Gouveia, 2018; Fdez-Sanromán et al., 2021). Additionally, when this technique is used in soils contaminated by hydrophobic organic compounds, solubilizing agents, such surfactants, are added to the washing fluid composition to increase the transport of the contaminant in the soil matrix (Boulakradeche et al., 2015; Mena Ramirez et al., 2015; Ramírez et al., 2015; Vieira dos Santos et al., 2017; Estabragh et al., 2018; Qiao et al., 2018; Ramadan et al., 2018; Melo Henrique et al., 2019; Suanon et al., 2020).

Among the low-solubility pesticides, HCH was the most used in the last half of the 20th and is formed from the reaction between chlorine gas and benzene. HCH consists of a mixture of several isomers, which are commonly α-HCH, β-HCH, γ-HCH, δ-HCH and ε –HCH (Calvelo Pereira et al., 2006; Santos et al., 2018; Vijgen et al., 2019; Waclawek et al., 2019). After the appearance of cases about the toxicity of this pesticide, causing serious environmental problems, it was banned for use in agriculture in most countries and today it is recognized as a persistent organic pollutant by the Stockholm Convention (Vijgen et al., 2011; Fernández et al., 2013; Madaj et al., 2018; Srivastava et al., 2019; Waclawek et al., 2019). Consequently, large deposits of unused HCHs pose a great danger due to their long residence time in the soil. The high potential risk exists not only in these places, but also in their surrounding environment, representing a source of secondary pollution of water and air (Wang et al., 2012; Torres et al., 2013; Alamdar et al., 2014; Camenzuli et al., 2016; Fang et al., 2017; Pokhrel et al., 2018; Gardes et al., 2021).

Most recently, in our previous work (Lopez-Vizcaino et al., 2017), has been reported that the application of electrochemically assisted technologies to remediate contaminated soil with 2,4-dichlorophenoxyacetic acid and oxyfluorfen that can lead to significant increases in soil temperature in prototype scale. Electrokinetic transport mechanisms

were the main responsible for the removal of pesticide in laboratory scale test, whereas volatilization was the main responsible for the removal of pesticide at prototype scale. It has also been highlighted that scale up is complex and that in making larger the EKSF setups, the controlling mechanisms change from electrokinetic to ohmic heating (Lopez-Vizcaino et al., 2017; Henrique et al., 2021). This means that EKSF should be re-engineered considering the most important inputs of another efficient soil remediation technology: Soil vapor extraction (SVE). In this later technology, pressurized air is injected in soil, where it drag pollution to extraction points, from which the pollutants are treated with a suitable gas remediation technology (Govindan and Moon, 2015; Henrique et al., 2021).

Differences between the rates and operation modes of EKSF and SVE are very important, but in applying EKSF, the presence of ohmic heating suggest that the smarter solution is the combination with SVE in the so called EKSF-SVE technology (Lageman et al., 2005; Simpanen et al., 2018). The resistance of the soil to the electric field depends on many factors such as water content of the soil and the composition of the soil and pore water, being the heating effect proportional to the resistance and to the square of the current intensity passed between anodes and cathodes. It is important to highlight that the rate of removal of contaminants from the soil also depends on this electrical current intensity, which, in addition, also fixes the rate of transport of species.

To evaluate the performance of this technology, in this work we have used an aged matrix containing a mixture of four isomers of hexachlorocyclohexanes (γ-HCH, ε-HCH, α-HCH, δ-HCH) integrated into a synthetic natural soil matrix compacted to simulate a real soil and special electrodic wells were prepared with caps that allow the injection and extraction of pressurized air. In addition, the soil was covered with a capillary barrier to prevent the spreading of pollution to atmosphere. Performance of EKSF with and without electrodes polarity reversal (1.0 V cm^{-1}) and applying two electric fields were compared in order to shed light on the way of integrating both technologies (1.0 and 3.0 V cm^{-1}).

2. Materials & methods

2.1. Chemical reagent and polluted soil

Analytical grade hexane (Sigma-Aldrich) and ethyl acetate (Scharlau) were used. Tap water (conductivity: 476 μS cm^{-1}, pH: 7.56) and sodium dodecyl sulfate (WWR Chemicals) were used to prepare the solubilizing solution from the wells. Deionized water (Millipore Milli-Q system, 18.2 MΩ cm, 25 °C) was used for the other solutions. A matrix of aged soil of low hydraulic conductivity contaminated with the isomers of lindane and natural soil free from contamination, collected in a quarry in the city of Toledo/Spain, were used. The main physical and chemical properties were measured according to the United States Department of Agriculture (USDA) (Vidal et al., 2020; Maldonado et al., 2021). The composition of the soil sample was Smectite 28%, Kaolinite 26%, Illite 20%, Feldspar 15%, Quartz 7%, Calcite 4% and organic content 0%. The soil showed particle size distribution (silt 68.2%, sand 26.9% and clay 4.9%) being classified as Silty Loam.

2.2. Experimental setup

The experimental installation consisted of methacrylate reactors with a capacity of 78.2 dm^3, feed tanks, peristaltic pumps, blowers to ventilate the atmosphere of the wells at predetermined times, hexane trap to retain the pollutant generated in the gas phase, tensiometers, thermocouples, dataloggers for data storage and energy sources.

Four different tests were performed: This included 1) a reference test in which only SVE is applied; 2) electrokinetic remediation tests with wells subjected to an electric field of 1 V cm^{-1} with polarity reversal; 3) 1 V cm^{-1} and 4) 3 V cm^{-1}.

The total soil volume was approximately 50 dm^3. The preparation of the soil in the reactor consisted of introducing a layer of gravel for

mechanical support and drainage and the distribution of three soil layers which individual layers were compacted into thick layers with a dry density of approximately 1.4 g cm^{-3} and a water content of 20% to reproduce its natural conditions, as described in previous works published by our groups (Vidal et al., 2020).

The layers were further scarified to ensure continuity and prevent the development of preferential flows during operation. Subsequently, the compacted soil was drilled to place the electrolyte wells, the contaminated soil in the center of the model (10 cm × 10 cm x 10 cm), and the instrumentation (tensiometers and thermocouples).

Finally, sealing of the system was performed to collect the contaminant generated from the evaporation flows. A 4 cm thick layer of sand was placed on top of the mock-up as an interface between the tested soil and the upper covering layer, also of 4 cm thick, made of bentonitic slurry. This bentonite layer acted as a barrier element to prevent uncontrolled diffuse vapor loss to the atmosphere. Over the bentonite, a new 4 cm thick layer of sand was placed, acting as a capillary barrier to reduce water evaporation from the bentonite. Also, the sealing includes the instrumentation of the wells to ensure that the electrolyte levels remain constant through the recirculation, the air inlet and outlet to collect the gaseous flows and the conductor wire of the electrode as shown in Figure S1.

A geotextile blanket was placed between the soil layers for reinforcement, separation, filtration, and drainage purposes. Graphite rod electrodes (2.5 cm × 2.5 cm × 17 cm) were used. Two wells were arranged in a row, facing each other, 30 cm apart. The pollution source was located exactly in the middle of the experimental set-up, equidistant from the wells. To start the operation, which lasted 15 days, the electrolyte wells were filled with a solution of sodium dodecyl sulfate (SDS) 10 g L^{-1}. Electric current was supplied by a Delta Elektronika power supply (MPL-3505 M, Minipa, 400 SM-8-AR ELEKTRONIKA DELTA BV). The system was operated in potenciostatic working mode for a period of 15 days. Air blowers were used to vent the atmosphere from the wells for a period of 10 min at predetermined intervals. The air flow was channeled into the hexane trap to collect the contaminants generated by evaporation for subsequent quantification. The hexane trap consisted of two bottles filled with hexane and placed in series.

Additionally, measurements of temperature, amount of electrolyte supplied to the wells, electric current, pH, conductivity, and the concentration of hexachlorocyclohexane isomers (γ-HCH, ε-HCH, α-HCH, δ-HCH), were performed. After 15 days, the soil treated was divided into three axial sampling points (z), as shown in Figure S2. For this, the soil was divided into six longitudinal positions (x) and three latitudinal positions (y), totaling 18 samples. Also, measurements of temperature, pH, conductivity, soil water suction and the concentration of hexachlorocyclohexane isomers (γ-HCH, ε-HCH, α-HCH, δ-HCH), were performed.

2.3. Characterization procedures and methods

Lindane and its isomers were identified and quantified employing a gas chromatography system with an electron capture detector (GC-ECD) (Thermo Fisher Scientific). The system was equipped with a TG-5MS capillary column (30 m × 0.25 mm × 0.25 mm), a 63 Ni micro electron-capture detector and a split/splitless injector. ChromCard software was employed by the GC-ECD. The flow rate of the He gas was 1.0 mL min^{-1}, while the injector temperature was maintained at 210 °C.

For this purpose, liquid-liquid (L-L) extraction of the liquid samples was performed with ethyl acetate in a ratio 1:1 v/v, employing 15 mL flasks, stirred in a vortex mixer (VV3 S040 multitube, VWR International, USA) by 5 min and centrifuged (CENCOM II P-elite, JP Selecta, Barcelona) at 3500 rpm for 10 min. The supernatant was collected and analyzed. Lindane and its isomers from soil were determined by extraction S-L mixture. S-L extraction with ethyl acetate in a ratio of 1 g of soil: 4 mL of solvent was carried out in 15 mL flasks. The S-L mixture was vigorously stirred for 5 min in a vortex mixer, sonicated for 10 min

(JP Selecta, Barcelona) and centrifuged at 3500 rpm for 10 min. The supernatant was collected and analyzed by GC-ECD. The hexane from the trap was collected at predetermined times and analyzed by GC-ECD to monitor the evaporation of the contaminants. For the determination of pH (Crison, GLP 22) and conductivity (Crison Ecmeter Basic 30+) in soil samples was performed according to the EPA 9045C standard method. This method consists of the mixture of 10 g of soil with 25 mL of deionized water (Millipore system Milli-Q, 18.2 MΩ cm, 25 °C) and magnetically agitated for 10 min. Soil water content and temperature were measured every 20 min (Figure S1). Water content measurements were performed through evaluation of the soil water suction, employing a set of model T5 tensiometers (UMS GmbH, Munich, Germany) inserted into the soil. Temperature measurements were performed employing ECT model thermocouples (Decagon Devices, Pullman, USA) inserted into the soil. All suction and temperature results were recorded with a model DL6 datalogger (UMS GmbH, Munich, Germany).

3. Results and discussion

Fig. 1 shows the electric current, accumulated charge and electro-osmotic flow changes observed for each of the three combined EKSF-SVE experimental systems evaluated over a period of fifteen days (Table S1). Results are also compared with a reference test in which only SVE is applied, and which was discussed in a previous work (results only shown here for comparative purposes). In all these tests, pressurized air was injected in the anode and extracted in the cathode using a system consisting of special caps and a capillary barrier on the surface of the soil, which prevents the uncontrolled emission of gases to the atmosphere and ensures that them are channeled in the desired direction.

As can be observed in the EKSF without polarity reversal, the higher is the electric gradient applied, the higher is the electric current recorded and, also, the higher volumes of water are needed to keep the electrolyte wells at constant level. The electric current increases up to a steady-state value, where it is kept during the rest of the tests. Regarding the water fluxes, it is important to consider that initially the flushing fluid was expected to be added in the anolyte well and extracted in the catholyte well, following the electro-osmotic flow direction, but the level of electrolyte decreases in both wells during the tests, consequently, it was needed the addition of flushing fluid in both to prevent their emptying. However, the volume added in the anolyte is much higher than that added in the catholyte confirming the electro-osmotic transport in the direction anode-cathode. The necessity of adding water can be explained because of the significance in the dragging of water vapor in the SVE process, which increases at higher electric fields applied. Comparing the EKSF with periodic polarity reversal with the single EKSF process (without polarity reversal), it can be seen that the electric current and the water required to be added is slightly higher. In addition, it results in higher charge passed through the mockup and a higher rate of water evaporation in the system with periodic polarity reversal.

The effect of the applied electric field on the soil water suction and temperature is shown in Fig. 2, where further details of the arrangement of tensiometers and thermometers can be found in Figure S3 and Table S1 of the Supplementary Material. As can be seen, the average temperate increases with the application of the electric field, being very important the change observed at the highest electric gradient. Suction values in the proximity of both the anode and the cathode are very low in all tests. These values suggest that water content does not become a problem in this technology, in which electrolyte wells are present and the level is kept constant throughout the experiments. The higher suction value detected in the anode at 3.0 V cm^{-1} indicates that electro-osmotic flux is more relevant at higher electric gradients, although an estimation cannot be done properly because of the very high evaporation rate. Opposite to these adequate water-content values in the proximity of the wells, the measurements made in a central point (far from the electrolytes well) indicates the important loss of water which
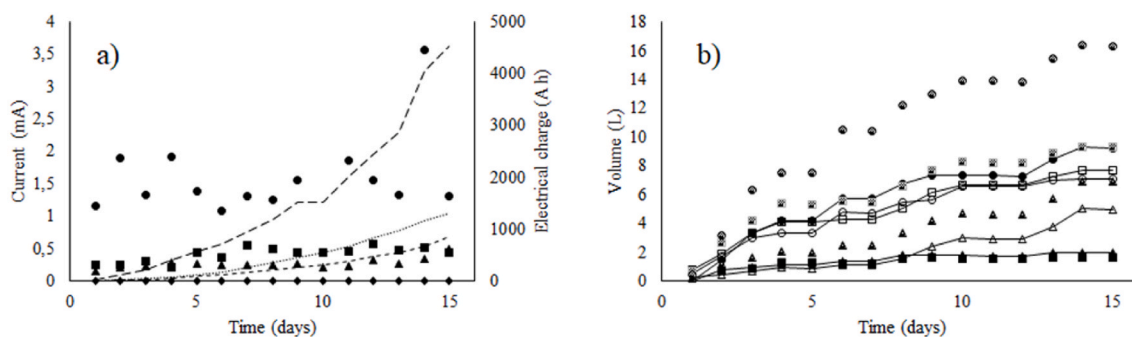
Fig. 1. (a) Time course of observed changes in electric current (markers) and accumulated electric charge (lines). Electric field: ◆ 0.0 V cm^{-1} (continuous line), ■ 1.0 V cm^{-1} reversible (point line), ▲ 1.0 V cm^{-1} (short dashed line) and ● 3.0 V cm^{-1} (long dashed line). (b) Electroosmotic flow during testing. Scale: ■ 1.0 V cm^{-1} reversible, ▲ 1.0 V cm^{-1} and ● 3.0 V cm^{-1}. Symbol filled with line: cathode; void symbol with line: anode; symbol filled with texture: balance.
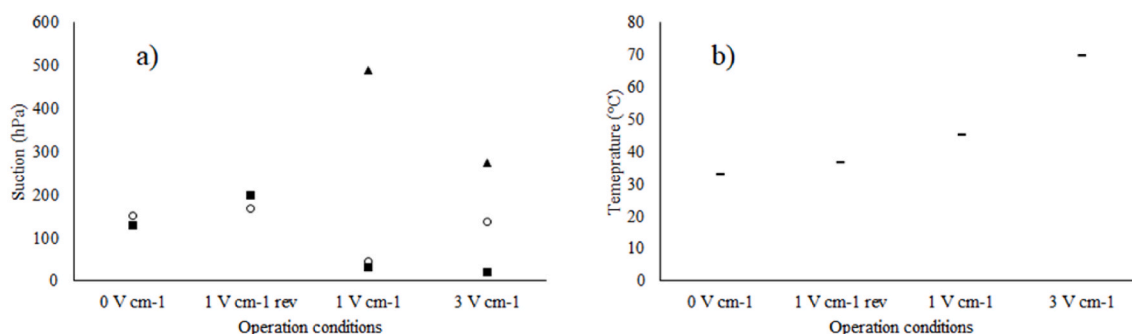
Fig. 2. a) Soil water suction: ■ cathode, ○ anode and ▲ middle; and b) average temperature (-) in the soil after the fifteen days of treatment.

apparently did not affect (but it might) to the performance of the system. Consequently, to ensure a good performance of the SVE-EKSF technology, a regular addition of flushing fluid should also be made at different points apart from the electrolyte wells.

Fig. 3 shows the profiles of pH and conductivity in the electrolyte wells and in the soil after the fifteen days of treatment. As expected, pH changes importantly in the electrolyte wells (2–13) and in the soil surrounding the wells (7–10), because of the transport of protons and
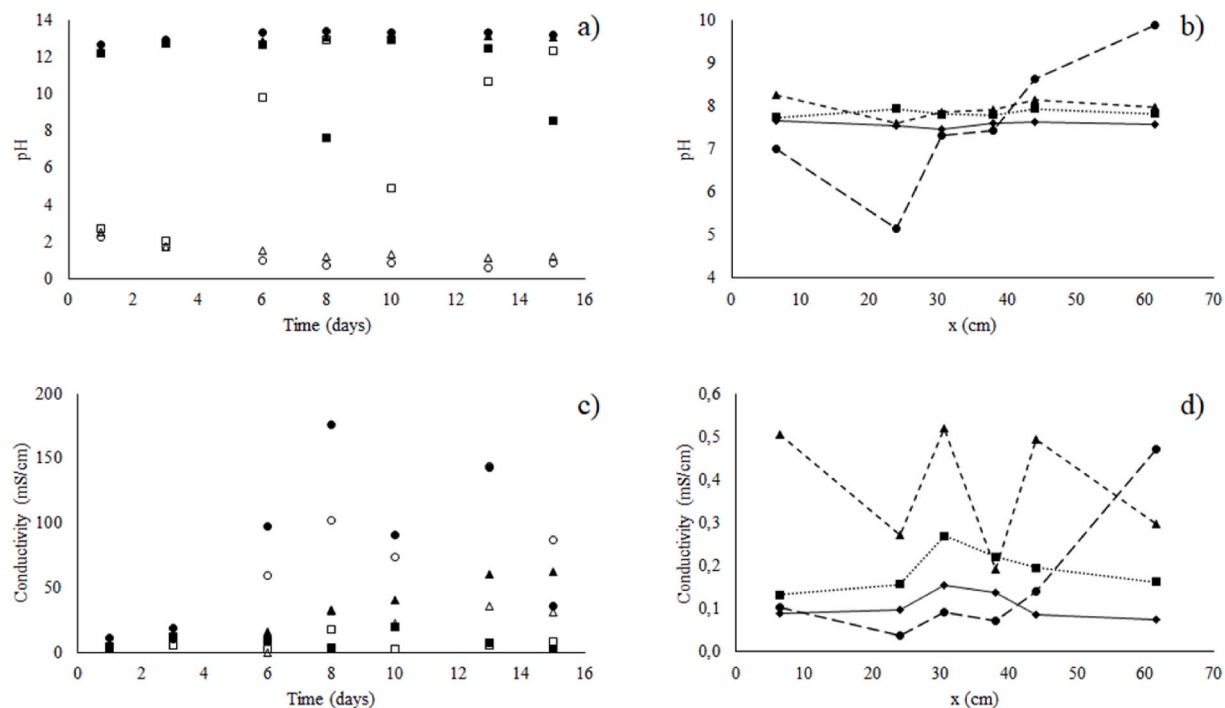

Fig. 3. pH and conductivity variations during the EKSF. (a) pH and (c) conductivity in the electrolyte wells (Symbol filled: cathode; void symbol: anode); and (b) pH and (d) conductivity in the soil after fifteen days of treatment. Electric field: ◆ 0.0 V cm^{-1} (continuous line), ■ 1.0 V cm^{-1} reversible (point line), ▲ 1.0 V cm^{-1} (short dashed line) and ● 3.0 V cm^{-1} (long dashed line).

hydroxyl ions (acidic and basic fronts). The effect is more relevant as the applied electric gradient is higher. Regarding conductivity, there is an important increase in both electrolyte wells and, also, a great dispersion in the soil matrix which indicates that electrokinetic processes are developing with a great extension and affecting the ions contained in the soil. The large increases observed in the wells can be explained in terms of the production of protons and hydroxyl ions during the oxidation and reduction of water, which are the main electrochemical processes expected on the surface of the electrodes. Also because of the migration of ions in the surroundings of the wells.

Fig. 4a and b shows the postmortem characterization (3-D maps) of two of the mockups evaluated in this work (1.0 V cm^{-1} with polarity reversibility and 3.0 V cm^{-1}, respectively) regarding the concentration of γ-HCH after fifteen days of treatment, showing each plot in vertical how the distribution change in each of the three layers in the vertical direction of the mockup.

Fig. 5 shows the changes in the top layer in the concentration of the four isomers (γ-HCH, ε-HCH, α-HCH, δ-HCH) in the mockup in which the 1 Vcm^{-1} tests was carried out.

As seen, pollutants distribute in a very different way although, considering the logarithmic scale, it is clear that the y and z axis mobility were almost negligible as compared with the x-axis mobility, what means that the systems can be approached with a maximum-gradient modelling simplification (1-D) as it was proposed in a previous manuscript in which the combination of EK with SVE was evaluated. In that work, it was also proposed a simplified model to evaluate the mobility of pure HCH in soil in which the distribution of the concentration of HCH in the soil was modelled according to the gaussian model shown in Eq (1), where m stands for the total amount of species i in the soil mockup (mg), S is the cross section area (m^2) and ρ_d is the dry density of soil (Kg dry soil m^{-3}), u_{eff} (m d^{-1}) is related to the dragging of the species i by the different induced flows (including not only the hydraulic flow but also electroosmotic flow, the electromigration and the electrophoresis) and D_{eff} (m^2 d^{-1}) is the effective diffusion/dispersion coefficient of this species under the experimental conditions. This coefficient is also influenced by the application of electric fields because the simplifications carried out may include in this diffusive transport the contribution from other transport processes not associated to exclusively to dragging (Selker and Or, 2019).

$$C_i(x,t) = \frac{m}{\rho_d S \sqrt{4\pi D_{eff} t}} e^{-\frac{(x - u_{eff} t)^2}{4 D_{eff} t}} \tag{1}$$

This equation satisfies the transport equation for each of the four HCH monitored, which takes the form shown in Eq. (2).

$$\frac{\partial C_i(x,t)}{\partial t} = D_{eff} \frac{\partial^2 C_i(x,t)}{\partial x^2} - u_{eff} \frac{\partial C_i(x,t)}{\partial x} \tag{2}$$

All experimental data measured regarding concentration of the four isomers HCH in the different positions were fitted to this model to obtain values of the two parameters. Only one value was used to fit u_{eff} in the four HCHs and different values were fitted for D_{eff}. Results obtained are shown in Fig. 6.

Regarding u_{eff}, it shows the effect of the dragging of pollutant by the electroosmotic flux, which is enhanced the higher the applied electric gradients are. Opposite, there is not an important influence of the application of low electric fields in the effective diffusion, with values which are like those obtained in the single SVE system and, opposite to what it could be expected, the effective diffusion decreases when the electric field applied was the highest. Fitting values obtained for the four isomers were very similar which suggest the robustness of the simplifications made. Values of the u_{eff} and D_{eff} are very low and indicates that transport of pollutants is slow. This explains the low concentrations of HCH contained in the electrolyte wells, whose time evolution is shown in Fig. 7a, for the gamma-HCH, and the final amounts collected in Fig. 7b for the four isomers and the three mockups (reference mockup did not contain electrolyte wells so there was not HCH collection).

A very important point that should be discussed is the transfer of HCH to the gas phase. Fig. 8 shows the amount of HCH volatilized in each test after the fifteen days of treatment and the onset gives the normalized volatilization rate in which the initial amount of each HCH is
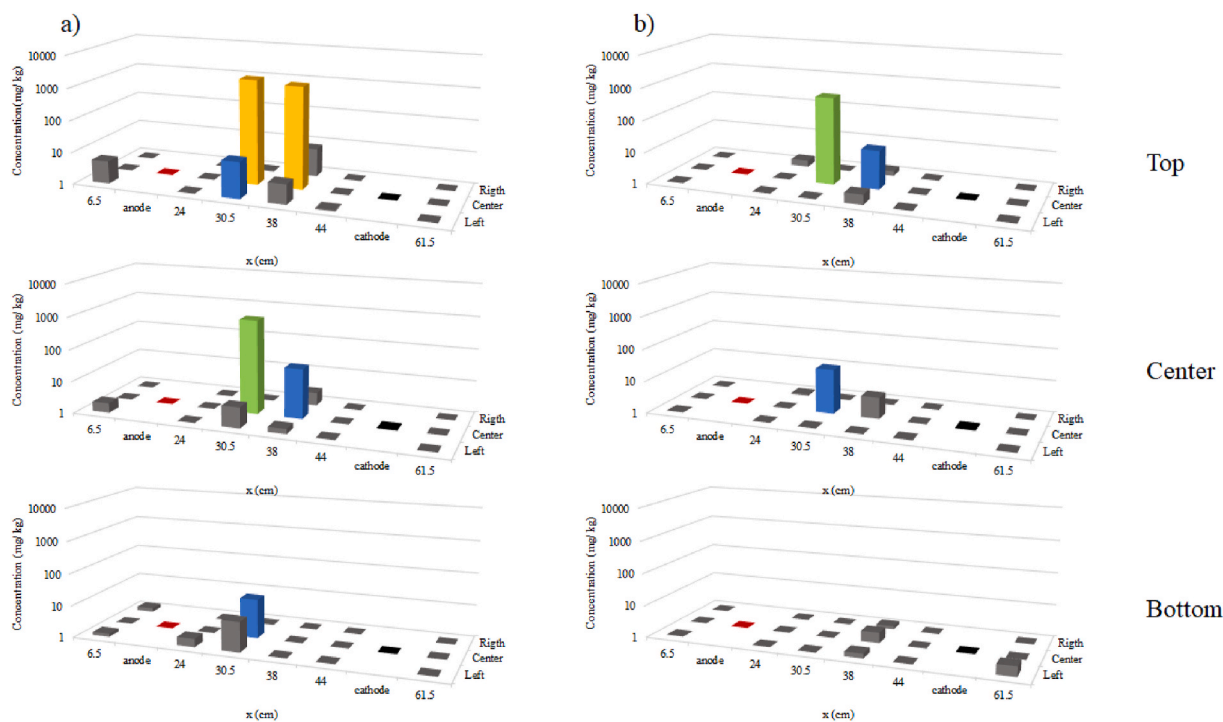

Fig. 4. 3-D scatter maps of γ-HCH after fifteen days. Colors: Grey: 1–10 mg kg^{-1}; Blue: 10–100 mg kg^{-1}; Green: 100–1000 mg kg^{-1}; Yellow: 1000–10000 mg kg^{-1}. Electric field: a) 1.0 V cm^{-1} with reversal polarity and b) 3.0 V cm^{-1}. (For interpretation of the references to colour in this figure legend, the reader is referred to the Web version of this article.)
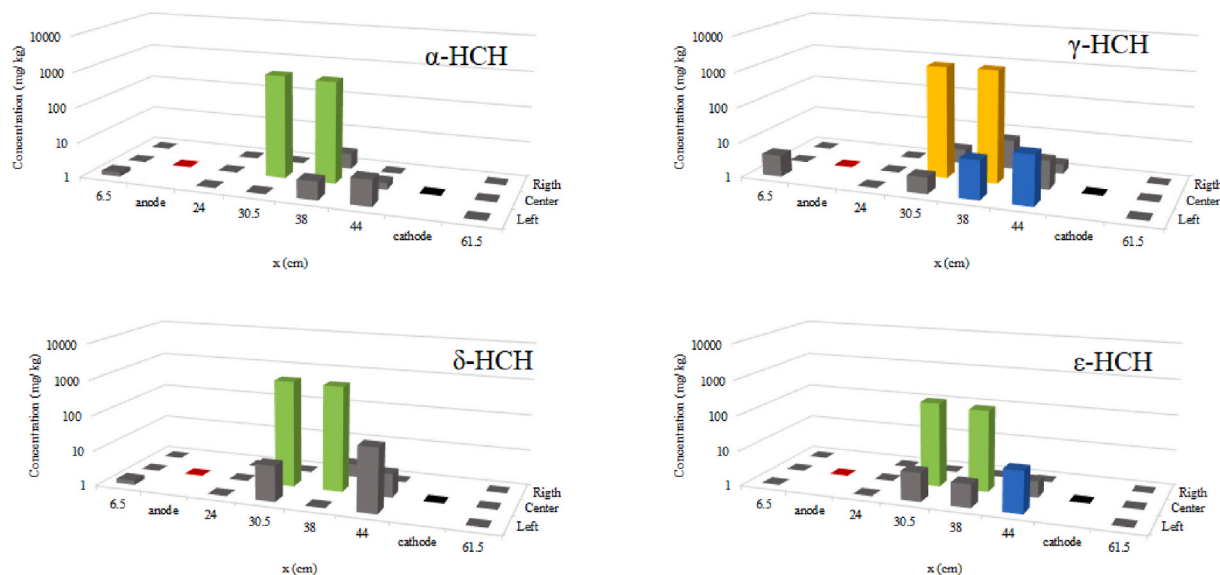
Fig. 5. Concentration of the four isomers in the top layer in the mockup in which 1.0 V cm^{-1} was applied. Colors: Grey: 1–10 mg kg^{-1}; Blue: 10–100 mg kg^{-1}; Green: 100–1000 mg kg^{-1}; Yellow: 1000–10000 mg kg^{-1}.
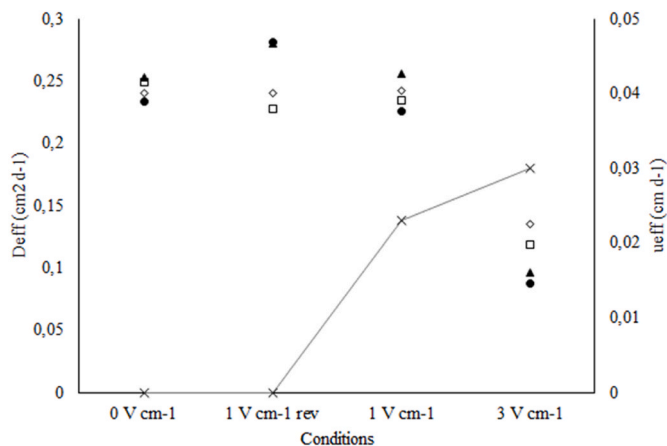
Fig. 6. Gaussian Parameters – Right y-axis: Effective diffusion (D_{eff}): (●) γ-HCH, (◇) ε-HCH, (□) α-HCH, (▲) δ-HCH; right y-axis: average pore water velocity (u_{eff}).

considered. As seen, the combined EKSF-SVE lead to higher volatilization of the HCH (except for the treatment in which the polarity is periodically reversed). These results can be explained in terms of the higher

temperature reached in the soil, which favors the volatilization of the isomers. This is especially important in the test made at 3.0 V cm^{-1}. It is important to highlight that, when data are normalized, all points lay over the same average values, with very low dispersion. This indicates the robustness of the experimental methodology used. Values of the volatilization of the four HCH with SVE technology was 0.0486 ± 0.0009 mg volatilized/mg contained/d like that of the SVE-ESKF with polarity reversal at 1.0 V cm^{-1} (0.0483 ± 0.0035 mg/mg/d) and lower than the 0.0496 ± 0.0021 mg/mg/d and 0.0664 ± 0.0024 mg/mg/d obtained for the 1.0 and 3.0 V cm^{-1} tests without polarity reversal.

Regarding the treatment results, Fig. 9 shows that efficiencies at low electric fields of the combined SVE-ESKSF does not differ importantly regarding the single SVE technology (68.05 ± 1.23% in the SVE vs 67.65 ± 4.83 and 69.46 ± 2.95 in the polarity reversal and single 1V cm^{-1} treatment). These results are similar that those previously reported in literature by Reddy et al. (2011), who investigated the EK-remediation of low permeability soil contaminated with pure lindane applying 1 V cm^{-1} of voltage gradient during 500 h. Results demonstrated that lindane was degraded by a direct electrochemical reducing process at the cathode, reaching a final removal percentage from 28% in the nearness of the anode to 80% close to the cathode. Recently, Vidal et al. (2020) reported that after 720 h of EKSF at 1.0 V cm^{-1} up to 70% of lindane is removed from the soil, being volatilization the main transport process. As observed in Fig. 9, these results are importantly enhanced at the highest 3.0 V cm^{-1} test in which a 92.94 ± 3.35% efficiency was
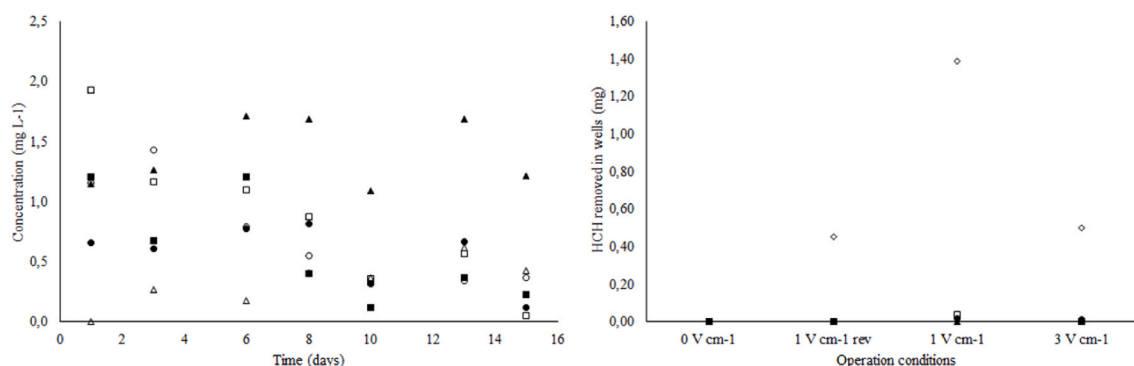

Fig. 7. a) γ-HCH concentration contained in electrolyte wells: (□) Anode 1.0 V cm^{-1} – Reversible, (■) Cathode 1.0 V cm^{-1} – Reversible, (△) Anode 1.0 V cm^{-1}, ▲ Cathode 1.0 V cm^{-1}, ○ Anode 3.0 V cm^{-1}, ● Cathode 3.0 V cm^{-1}; b) Final mass of isomers collected in the wells: ● γ-HCH; ◇ ε-HCH; □ α-HCH; ▲ δ-HCH.
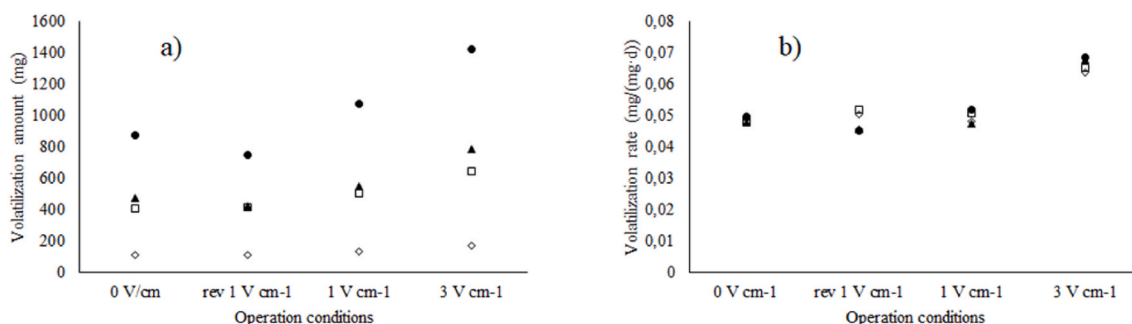
Fig. 8. a) amount of HCH volatilized in each test after the fifteen days of treatment and b) normalized volatilization rate. Isomers: ● γ-HCH; ◇ ε-HCH; □ α-HCH; ▲ δ-HCH.
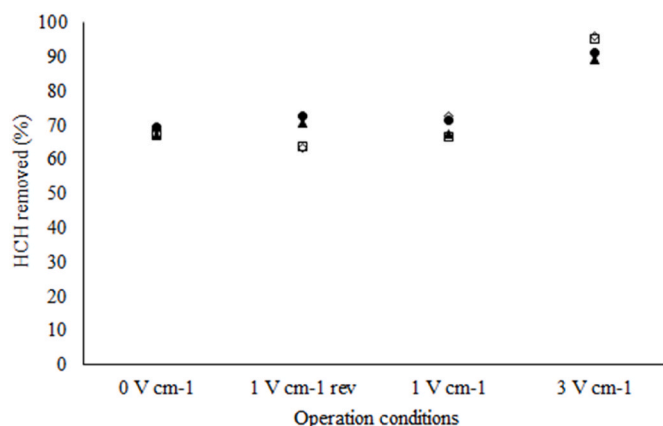

Fig. 9. Removal efficiency of HCH isomers in different electric fields. Isomers: ● γ-HCH; ◇ ε-HCH; □ α-HCH; ▲ δ-HCH.

reached.

Therefore, the combination of EKSF and SVE can be positive, but it is required the application of high electric fields to promote a higher temperature in the system which improves the volatilization of the HCH contained in the system. This heating can affect the morphology and physicochemical properties of the soil, but this does not seem to affect negatively to the performance of the system. In fact, EK transport is enhanced with the application of electric fields, but these transport processes are much slower than the volatilization processes which are the primary in this system. Hence collection of species in the electrolyte wells is negligible as compared to the compound dragged with air by the SVE although the temperature increase reveals a good performance.

4. Conclusions

From this work, the following conclusions can be drawn:

- Combination of EKSF with SVE can efficiently extract the HCH isomers reaching a removal of more than 90% after 15 days of treatment. Higher electric field applied affect the pH and conductivity profiles of the soil but also of the electrolyte reservoirs. On the other hand, when 1 V cm^{-1} is applied with polarity reversal the alkaline and acidic front is less evident both in the soil and in the reservoirs.
- Application of higher electric gradients (3 V cm^{-1}) contributed to an increase in the mobility of the HCH by EK transport mainly in the direction anode-cathode, but more importantly promoted the stripping of pollutants made by the SVE process, due to the raise of temperature.
- No relevant differences are observable between the performance of the technologies with the four HCH isomers, and similar average

pore water velocity and effective diffusion are predicted by a simple 1-D transport model.

Credit author statement

João Miller de Melo Henrique: Investigation; Writing – original draft; Methodology; Data curation. Julia Isidro, Rubén Lopez-Vizcaíno, Angel Yustres: Investigation; Validation; Formal analysis; writing – review and edition. Vicente Navarro, Cristina Sáez: Supervision; Validation; Formal analysis; writing – review and edition. Elisama V. Dos Santos: Conceptualization; Funding acquisition; Supervision; writing – review and edition. M.A. Rodrigo: Conceptualization; Funding acquisition; Supervision; writing - review and edition.

Declaration of competing interest

The authors declare that they have no known competing financial interests or personal relationships that could influence the work reported in this paper.

Appendix A. Supplementary data

Supplementary data to this article can be found online at https://doi.org/10.1016/j.chemosphere.2022.134052.

References

Alamdar, A., Syed, J.H., Malik, R.N., Katsoyiannis, A., Liu, J., Li, J., Zhang, G., Jones, K. C., 2014. Organochlorine pesticides in surface soils from obsolete pesticide dumping ground in Hyderabad City, Pakistan: contamination levels and their potential for air–soil exchange. Sci. Total Environ. 470–471, 733–741.

Araújo, M.M., Ignatius, S.G., Oliveira, A.O., Oliveira, S.S., Fertonani, F.L., Paste, I.A., 2016. Thermal desorption of HCH. J. Therm. Anal. Calorim. 123, 1019–1029.

Boulakradeche, M.O., Akretche, D.E., Cameselle, C., Hamidi, N., 2015. Enhanced electrokinetic remediation of hydrophobic organics contaminated soils by the combination of non-ionic and ionic surfactants. Electrochim. Acta 174, 1057–1066.

Calvelo Pereira, R., Camps-Arbestain, M., Rodríguez Garrido, B., Macías, F., Monterroso, C., 2006. Behaviour of α-, β-, γ-, and δ-hexachlorocyclohexane in the soil–plant system of a contaminated site. Environ. Pollut. 144, 210–217.

Camenzuli, L., Scheringer, M., Hungerbühler, K., 2016. Local organochlorine pesticide concentrations in soil put into a global perspective. Environ. Pollut. 217, 11–18.

Cameselle, C., Gouveia, S., 2018. Electrokinetic remediation for the removal of organic contaminants in soils. Curr. Opin. Electrochem. 11, 41–47.

Chen, Z., Tang, X., Qiao, W., Puentes Jácome, L.A., Edwards, E.A., He, Y., Xu, J., 2020. Nanoscale zero-valent iron reduction coupled with anaerobic dechlorination to degrade hexachlorocyclohexane isomers in historically contaminated soil. J. Hazard Mater. 400, 123298.

Dominguez, C.M., Checa-Fernandez, A., Romero, A., Santos, A., 2021. Degradation of HCHs by thermally activated persulfate in soil system: effect of temperature and oxidant concentration. J. Environ. Chem. Eng. 9, 105668.

dos Santos, E.V., Souza, F., Saez, C., Canizares, P., Lanza, M.R., Martinez-Huitle, C.A., Rodrigo, M.A., 2016. Application of electrokinetic soil flushing to four herbicides: a comparison. Chemosphere 153, 205–211.

Estabragh, A.R., Lahoori, M., Ghaziani, F., Javadi, A.A., 2018. Electrokinetic remediation of a soil contaminated with anthracene using different surfactants. Environ. Eng. Sci. 36, 197–206.

Fang, Y., Nie, Z., Die, Q., Tian, Y., Liu, F., He, J., Huang, Q., 2017. Organochlorine pesticides in soil, air, and vegetation at and around a contaminated site in southwestern China: concentration, transmission, and risk evaluation. Chemosphere 178, 340–349.

Fdez-Sanromán, A., Pazos, M., Rosales, E., Sanromán, M.Á., 2021. Prospects on integrated electrokinetic systems for decontamination of soil polluted with organic contaminants. Curr. Opin. Electrochem. 27.

Fernández, J., Arjol, M.A., Cacho, C., 2013. POP-contaminated sites from HCH production in Sabiñánigo, Spain. Environ. Sci. Pollut. Control Ser. 20, 1937–1950.

Gardes, T., Portet-Koltalo, F., Debret, M., Copard, Y., 2021. Historical and post-ban releases of organochlorine pesticides recorded in sediment deposits in an agricultural watershed, France. Environ. Pollut. 288, 117769.

Gomes, H.I., Dias-Ferreira, C., Ribeiro, A.B., 2012. Electrokinetic remediation of organochlorines in soil: enhancement techniques and integration with other remediation technologies. Chemosphere 87, 1077–1090.

Govindan, M., Moon, I.-S., 2015. Uncovering results in electro-scrubbing process toward green methodology during environmental air pollutants removal. Process Saf. Environ. Protect. 93, 227–232.

Hahladakis, J.N., Latsos, A., Gidarakos, E., 2016. Performance of electroremediation in real contaminated sediments using a big cell, periodic voltage and innovative surfactants. J. Hazard Mater. 320, 376–385.

Henrique, J.M.d.M., Cañizares, P., Saez, C., Vieira dos Santos, E., Rodrigo, M.A., 2021. Relevance of gaseous flows in electrochemically assisted soil thermal sremediation. Curr. Opin. Electrochem. 27.

Lageman, R., Clarke, R.L., Pool, W., 2005. Electro-reclamation, a versatile soil remediation solution. Eng. Geol. 77, 191–201.

Liu, B., Li, G., Mumford, K.G., Kueper, B.H., Zhang, F., 2020. Low permeability zone remediation of trichloroethene via coupling electrokinetic migration with in situ electrochemical hydrodechlorination. Chemosphere 250, 126209.

Lopez-Vizcaino, R., Risco, C., Isidro, J., Rodrigo, S., Saez, C., Canizares, P., Navarro, V., Rodrigo, M.A., 2017. Scale-up of the electrokinetic fence technology for the removal of pesticides. Part II: does size matter for removal of herbicides? Chemosphere 166, 549–555.

Madaj, R., Sobiecka, E., Kalinowska, H., 2018. Lindane, kepone and pentachlorobenzene: chloropesticides banned by Stockholm convention. Int. J. Environ. Sci. Technol. 15, 471–480.

Maldonado, S., López-Vizcaíno, R., Rodrigo, M.A., Cañizares, P., Navarro, V., Roa, G., Barrera, C., Sáez, C., 2021. Scale-up of electrokinetic permeable reactive barriers for the removal of organochlorine herbicide from spiked soils. J. Hazard Mater. 417, 126078.

Melo Henrique, J.M., Andrade, D.C., Barros Neto, E.L., Silva, D.R., Santos, E.V., 2019. Solar-powered BDD-electrolysis remediation of soil washing fluid spiked with diesel. J. Chem. Technol. Biotechnol. 94, 2999–3006.

Mena Ramirez, E., Villasenor Camacho, J., Rodrigo, M.A., Canizares, P., 2015. Combination of bioremediation and electrokinetics for the in-situ treatment of diesel polluted soil: a comparison of strategies. Sci. Total Environ. 533, 307–316.

Minghui, Z., Zhicheng, B., Xiaobai, X., Keou, W., 1996. Formation of polychlorinated dibenzo-p-dioxins and dibenzofurans from the pyrolysis of hexachlorocyclohexane in the presence of iron(III) oxide. Chemosphere 32, 595–602.

Munoz-Morales, M., Braojos, M., Saez, C., Canizares, P., Rodrigo, M.A., 2017. Remediation of soils polluted with lindane using surfactant-aided soil washing and electrochemical oxidation. J. Hazard Mater. 339, 232–238.

Phillips, T.M., Seech, A.G., Lee, H., Trevors, J.T., 2005. Biodegradation of hexachlorocyclohexane (HCH) by microorganisms. Biodegradation 16, 363–392.

Pokhrel, B., Gong, P., Wang, X., Chen, M., Wang, C., Gao, S., 2018. Distribution, sources, and air–soil exchange of OCPs, PCBs and PAHs in urban soils of Nepal. Chemosphere 200, 532–541.

Qiao, W., Ye, S., Wu, J., Zhang, M., 2018. Surfactant-enhanced electroosmotic flushing in a trichlorobenzene contaminated clayey soil. Groundwater 56, 673–679.

Ramadan, B.S., Sari, G.L., Rosmalina, R.T., Effendi, A.J., Hadrah, 2018. An overview of electrokinetic soil flushing and its effect on bioremediation of hydrocarbon contaminated soil. J. Environ. Manag. 218, 309–321.

Ramírez, E.M., Jiménez, C.S., Camacho, J.V., Rodrigo, M.A.R., Cañizares, P., 2015. Feasibility of coupling permeable bio-barriers and electrokinetics for the treatment of diesel hydrocarbons polluted soils. Electrochim. Acta 181, 192–199.

Reddy, K.R., Darko-Kagya, K., Al-Hamdan, A.Z., 2011. Electrokinetic remediation of pentachlorophenol contaminated clay soil. Water, air. Soil Pollut. 221, 35–44.

Risco, C., Rubi-Juarez, H., Rodrigo, S., Lopez-Vizcaino, R., Saez, C., Canizares, P., Barrera-Diaz, C., Navarro, V., Rodrigo, M.A., 2016. Removal of oxyfluorfen from spiked soils using electrokinetic soil flushing with the surrounding arrangements of electrodes. Sci. Total Environ. 559, 94–102.

Rodrigo, M.A., dos Santos, E.V., 2020. Electrochemically Assisted Remediation of Contaminated Soils. Springer.

Rodrigo, M., Mena, E., Ruiz, C., Risco, C., Villaseñor, J.J., Sáez, C., Navarro, V., Cañizares, P., 2014a. Combined electrokinetic soil flushing and bioremediation for the treatment of spiked soils polluted with organics. Chem. Eng. Trans. 41, 109–114.

Rodrigo, M.A., Oturan, N., Oturan, M.A., 2014b. Electrochemically assisted remediation of pesticides in soils and water: a review. Chem. Rev. 114, 8720–8745.

Santos, A., Fernández, J., Guadaño, J., Lorenzo, D., Romero, A., 2018. Chlorinated organic compounds in liquid wastes (DNAPL) from lindane production dumped in landfills in Sabiñanigo (Spain). Environ. Pollut. 242, 1616–1624.

Selker, J., Or, D., 2019. Soil Hydrology and Biophysics.

Simpanen, S., Yu, D., Mäkelä, R., Talvenmäki, H., Sinkkonen, A., Silvennoinen, H., Romantschuk, M., 2018. Soil vapor extraction of wet gasoline-contaminated soil made possible by electroosmotic dewatering–lab simulations applied at a field site. J. Soils Sediments 18, 3303–3309.

Song, Y., Lei, C., Yang, K., Lin, D., 2021. Iron-carbon material enhanced electrokinetic remediation of PCBs-contaminated soil. Environ. Pollut. 290, 118100.

Srivastava, V., Srivastava, T., Kumar, M.S., 2019. Fate of the persistent organic pollutant (POP)Hexachlorocyclohexane (HCH) and remediation challenges. Int. Biodeterior. Biodegrad. 140, 43–56.

Suanon, F., Tang, L., Sheng, H., Fu, Y., Xiang, L., Herzberger, A., Jiang, X., Mama, D., Wang, F., 2020. TW80 and GLDA-enhanced oxidation under electrokinetic remediation for aged contaminated-soil: does it worth? Chem. Eng. J. 385, 123934.

Torres, J.P.M., Fróes-Asmus, C.I.R., Weber, R., Vijgen, J.M.H., 2013. HCH contamination from former pesticide production in Brazil—a challenge for the Stockholm Convention implementation. Environ. Sci. Pollut. Control Ser. 20, 1951–1957.

Usman, M., Tascone, O., Faure, P., Hanna, K., 2014. Chemical oxidation of hexachlorocyclohexanes (HCHs) in contaminated soils. Sci. Total Environ. 476–477, 434–439.

Usman, M., Tascone, O., Rybnikova, V., Faure, P., Hanna, K., 2017. Application of chemical oxidation to remediate HCH-contaminated soil under batch and flow through conditions. Environ. Sci. Pollut. Control Ser. 24, 14748–14757.

Vidal, J., Carvela, M., Saez, C., Cañizares, P., Navarro, V., Salazar, R., Rodrigo, M.A., 2020. Testing different strategies for the remediation of soils polluted with lindane. Chem. Eng. J. 381.

Vieira dos Santos, E., Sáez, C., Cañizares, P., Martínez-Huitle, C.A., Rodrigo, M.A., 2017. Reversible electrokinetic adsorption barriers for the removal of atrazine and oxyfluorfen from spiked soils. J. Hazard Mater. 322, 413–420.

Vijgen, J., Abhilash, P.C., Li, Y.F., Lal, R., Forter, M., Torres, J., Singh, N., Yunus, M., Tian, C., Schäffer, A., Weber, R., 2011. Hexachlorocyclohexane (HCH) as new Stockholm Convention POPs—a global perspective on the management of Lindane and its waste isomers. Environ. Sci. Pollut. Control Ser. 18, 152–162.

Vijgen, J., de Borst, B., Weber, R., Stobiecki, T., Forter, M., 2019. HCH and lindane contaminated sites: European and global need for a permanent solution for a long-time neglected issue. Environ. Pollut. 248, 696–705.

Virkutyte, J., Sillanpää, M., Latostenmaa, P., 2002. Electrokinetic soil remediation — critical overview. Sci. Total Environ. 289, 97–121.

Waclawek, S., Silvestri, D., Hrabak, P., Padil, V.V.T., Torres-Mendieta, R., Waclawek, M., Cernik, M., Dionysiou, D.D., 2019. Chemical oxidation and reduction of hexachlorocyclohexanes: a review. Water Res. 162, 302–319.

Wang, X.-p., Sheng, J.-j., Gong, P., Xue, Y.-g., Yao, T.-d., Jones, K.C., 2012. Persistent organic pollutants in the Tibetan surface soil: spatial distribution, air–soil exchange and implications for global cycling. Environ. Pollut. 170, 145–151.